SVU-International Journal of Engineering Sciences and Applications (2023) 4(2): 76-83
Print ISSN 2785-9967| Online ISSN 2735-4571
DOI 10.21608/SVUSRC.2023.195243.1107

High Robust Control Model of High Step Up Three Phase Y Source Inverters based on Model Predictive Control

Mohamed A. Ismeil[1,2,]*, Omima Abdelaal[3], M.Orabi[3]
(https://orcid.org/0000-0002-9885-8501)

Abstract Considering the spread spectrum problem of finite-control-set model predictive control (FCS-MPC), a Model predictive control technique for the quasi Y-Source Inverter with RL load to enhance the following effectiveness of the tracking efficiency by using the cost function. The controller achieves optimal voltage vector by minimizing the errors in one cost function, the weighting factor for each absolute error has been used, the system has been tested under dynamic load change, and fast response has been achieved using FCS- MPC for the output load current. Moreover, the controller maintains capacitor voltage to be constant with no minimum value over/under-shoot. The MPC model has been created and then the whole system has been validated under MPC based on MATLAB SIMULINK Software. The results of output currents, capacitors voltages, and inductor current have been presented and detailed discussed The results show how fast the MPC is in tracking the reference signal.

Keywords: Z-Source Inverter, Y-Source Impedance network; Multivariable Model Predictive Control.

1. Introduction

The dream of reducing carbon dioxide emissions in the atmosphere will remain one of the most important aspirations pursued by all countries, especially the major industrial countries. One of the most important ways to reduce emissions is to use clean energy, such as wind and solar energy. To start with, the fast decrease in environmentally friendly power costs.

Levelized cost of electricity (LCOE) for PV plants According to 2021 statistics decreased by 13%. As for cost statistics, it swallowed USD 0.048/kWh in 2021, but in the previous year, it reached USD 0.055/kWh however, the concentrating solar power (CSP), deployment remains limited and the cost is around 7% higher than the average in 2020 [1]. Since 2010, a large number of solar energy systems have been sold, and the number of units reached 180 million units that are off-grid systems, including 150 million units of the small type and 30 million units of sun-based home frameworks. The market for offline systems grew by about 13% in 2019. Additionally, environmentally friendly power (by and large hydropower) gave either total or general, the total number of micro-grid reached 19,000. These related solar systems have captured the attention of many countries, especially in some countries in Africa and Asia **[2]**. Among the new and renewable sources, solar energy recorded the highest use at 39%, followed by wind energy at 31%, while a small part, about 3%, comes from new nuclear energy [2].

Received: 2**1** Feb.y 2023/ Accepted: 9 March 2023
* Corresponding Author Mohamed A. Ismeil,, mohamedismeil@eng.svu.edu.eg
Other Author Name, E-mail
1. Electrical Engineering Department, Faculty of Engineering, King Khalid University, Abha 61411, Saudi Arabia
2. 2Electrical Engineering Department, Faculty of Engineering, South Valley University, Egypt.
3. APEAC, Faculty of Enginering. Aswan University ,Egypt

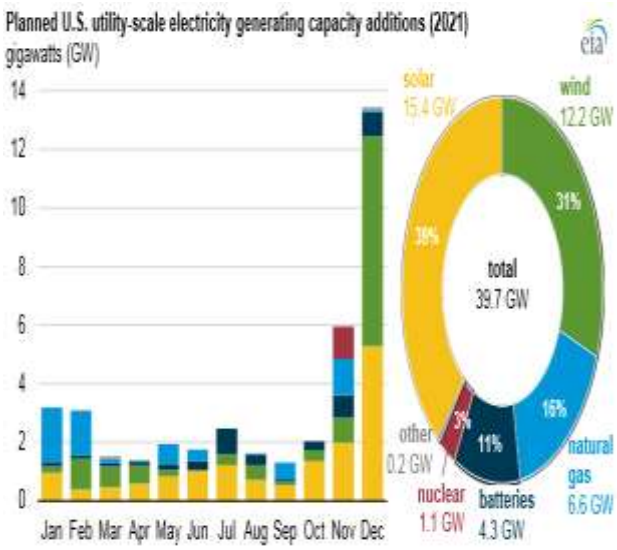

Fig. 1: Electrical generation capacity addition in USA 2021 [2].

The interface between the renewable energy resources and the different load has the optimal role to take advantage of renewable energy. The interface units have been presented as two-stage topologies or single-stage topologies. The two-stage start with any of the family of DC-DC converters and are then followed by the second stage which is DC/AC inverter. It is worth mentioning that this topology has limitations such as the large counts of components and the complication of control. The single-stage topologies have been presented to overcome the limitation of two-stage topologies such as the counts of components and the cost. The first topology of the single stage uses a large transformer to step up the voltage which means it has a large size [3].

The impedance inverters have been presented as single-stage with the ability to boost without using additional switches. The Z-source inverter (ZSI) that presents in Fig. 2 [4] has X-shape passive elements which are two capacitors, two inductors, and one diode beside the traditional inverter switches. The idea of this inverter is to use the available switches to extract an extra state to be the ninth state. It can be done by turning on two switches on the same leg or turning on all switches. Despite the advantages offered by this inverter, it faces many problems, including high voltage stress of semiconductor gadgets, invert recuperation issue of diodes, low boosting, Discontinuous Conduction Mode (DCM), and inrush current problem. One of the most important advantages of the Z-Source Inverter is that the output distortion is small and it has high reliability. It is worth noting that Z-Source inverters have witnessed great leaps in development since the first version of them was presented in 2003. The development was on two levels, the first level was in the power circuit, and the second level was from the point of view of control, whether logical or digital control so that a strong issue of the inverter with high performance and higher efficiency can be created.

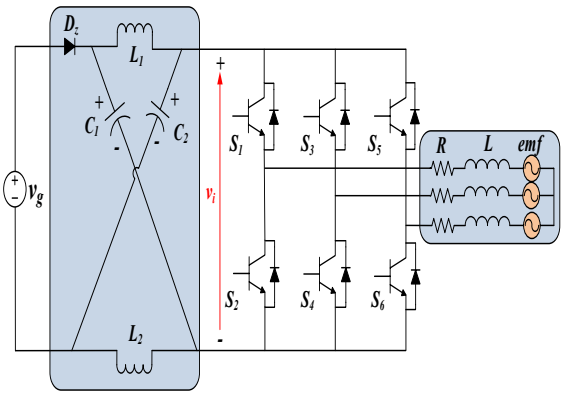

Fig. 2: Z Source invretr .

Quazi Z-source inverter (QZSI) shown in Fig.3, has been presented to solve the problem of DCM and inrush current [5]. The main limitation of the Z-Source inverter is that it has a low boost factor so, many improvements for Z-source have been presented such as switched inductor/capacitor Z-source inverter, and high gain extended Z-source inverter, Although the inverter increased its boosting factor, the number of components used also increased, and the stress on them increased. The Switched Inductor (SL-qZSI shown in Fig.4 has been presented to solve the problem of the lack of boosting [6-8].

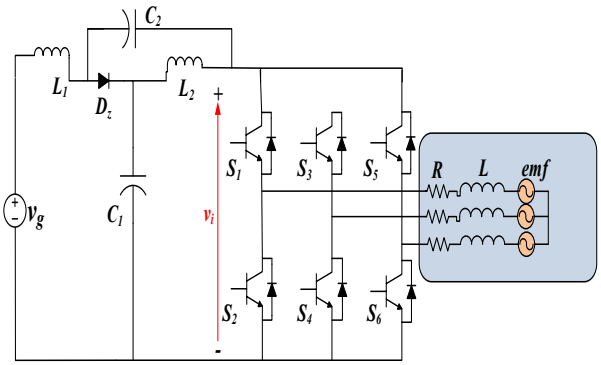

Fig. 3: Quasi Z -Source invertr .

However, the problem of the inrush current and the lack of boosting has been solved in Improved Switched Inductor ZSI (ISL-ZSI) [9]. the T-source inverter is recently acquainted with beating the issues of Z-source inverter. T-Source Inverter is like Z-Source aside from the utilization of high recurrence low spillage inductance transformer and one Capacitance.

It has low responsive parts in contrast and ordinary ZSI [10]. Because of this, productivity enormously increments. The TSI geography requires an extremely low spillage inductance transformer which ought to be made with high accuracy. In such a manner, the quantity of LC components is decreased in light of the fact that main the transformer and the capacitor are required. The T-Source Inverter geography capacities as a normal DC interface between the source and inverter. It isn't the same as the conventional Z-Source Inverter circuits.

Utilization of a transformer with other than a 1:1 transformer proportion considers a difference in yield voltage Z-source converters, as analyzed with the voltage coming about because of the shoot-through record or the adjustment record.

Two operating modes exist in the T-source inverter. One is active mode and the other is Shoot-through mode. The difference between T-Source and Z-source is that the L-C tank circuit has been replaced by T-network, and the T-network has the samefunction concerning the boosting vai shot through between two switches in one leg or all legs. [10].

The highlights of T - Source inverter are as per the following:

- Low receptive parts in contrast with ordinary Z-source inverter.
- Utilization of a typical voltage wellspring of the inactive plan.
- Limit the quantity of switching devices.
- No requirements for dead time.
- The inductor diminishes the inrush current and sounds in the inrush current.

But there are disadvantages in the T source inverter there are discontinuous input current and Start-up inrush current. To solve the problems related to the inverter, the Y Source inverter appeared in 2014 as a flexible design which is shown in Fig.5. [11]. The Y network utilizes a tightly coupled transformer with three windings. By getting the shoot-through range while keeping a higher boost, the inverter can work at a higher modulation index, in this way limiting switching device stress and giving better result power quality. Moreover, the inverter has more levels of opportunities for setting the voltage gain and modulation index than other traditional impedance-source organizations. Y source inverter Its benefit has for sure been demonstrated higher than other classical impedance networks even with a more small shoot-through duty cycle utilized.

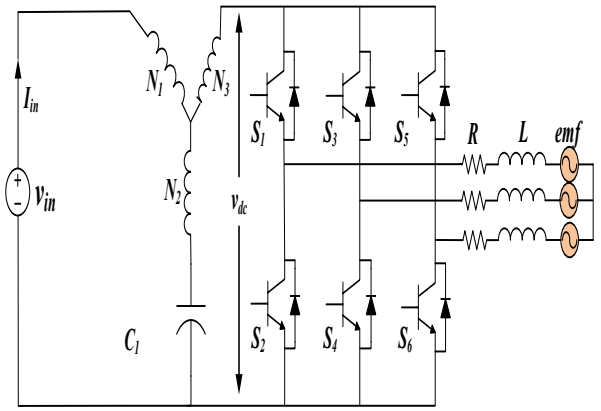

Fig. 5: Y -Source invertr .

The use of many types of renewable energy has led to the spread of the use of the quasi Y Source inverters (qYSIs) because of their advantages. Among the applications in which the qYSI inverter can be used are microgrids and uninterruptible power supplies (UPS), with multi-level output and also a fixed frequency when connected to the grid under conditions of continuous load change, as shown in Fig .6 [12-16].

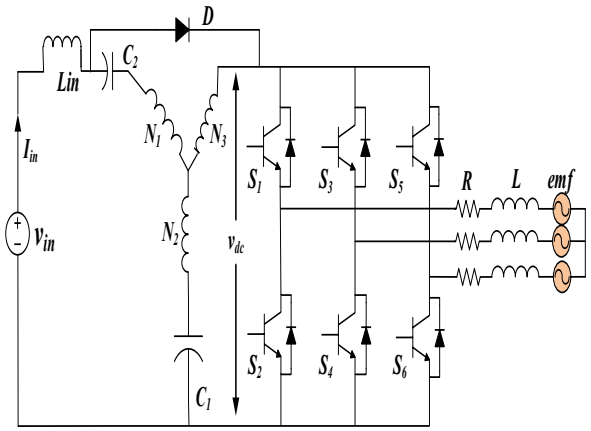

Fig. 6: Quasi Y -Source invertr .

Several topologies have been presented concern with Y-Source topology Table I summarized the total stress and going for each topology.

Table: I comparison between different Y-Source Inverter topologies

Parameter for comparison	Y-Source	Extended quasi Y-Source [17]	quasi Y-Source [16]
k	$\frac{N3+N1}{N3-N2}$	$\frac{N3+N1}{N3-N2}$	$\frac{N1+N2}{N2-N3}$
B=V_{dc}/Vin	$\frac{1}{1-kd_{st}}$	$\frac{1}{1-(k+1)d_{st}}$	$\frac{1}{1-kd_{st}}$
V_D	$(K-1)BV_{in}$	$-KBV_{in}$	$(K-1)BV_{in}$
V_{C1}	$(1-d_{st})BV_{in}$	$(1-d_{st})BV_{in}$	$(1-d_{st})BV_{in}$
V_{C2}	*NA*	$Kd_{st}BV_{in}$	$(K-1)d_{st}BV_{in}$
I_{ST}	$\frac{KP}{V_{in}}$	$\frac{(K+1)P}{V_{in}}$	$\frac{KP}{V_{in}}$
iN1,peak	$P/V_{in}(1-dst)$	P/V_{in}	$P/V_{in}(1-dst)$
iN2,peak	$\frac{KP}{V_{in}}$	$\frac{(K+1)P}{V_{in}}$	$\frac{KP}{V_{in}}$
iN3,peak	KP/V_{in}	$(K+1)P/V_{in}$	KP/V_{in}

2. Quasi Y-inverter Modes

The theory of inverter operation is summarized in that it works in two modes shoot through zero state and non-shoot through and it contains 9 states 6 of which are active, 2 zero and 1 zero, by shoot through zero state. The shoot through equivalent circuit is shown in Fig.7 a

In the shoot through mode the inverter equations can be presented as:

The inductor voltage:

$$L\frac{di}{dt} = V_{in} + V_{c2} - V_{c1}(K) * \left(1 + \frac{n1+n2}{n3-n2}\right) + r_l i_l \quad (1)$$

The capacitor voltage

$$V_{c1}(K) = \frac{n3-n2}{n1} V_{Lp} \quad (2)$$

Equation (2) can be rearranged as:

$$C_1 \frac{dvc1(K)}{dt} = \frac{n3-n2}{n1} V_{Lp} \quad (3)$$

In the non- shoot through mode shown in Fig.7 b, the inverter equations can be presented as:

The inductor voltage :

$$L\frac{di}{dt} = V_{in} + V_{c2} - V_{c1}(K) - \frac{n1+n2}{n1+n3} * V_{c2} + r_l i_l \quad (4)$$

The DC input voltage

$$V_{dc} = V_{c1}(K) + V_{c2} - \frac{n1+n2}{n1} * V_{Lp} \quad (5)$$

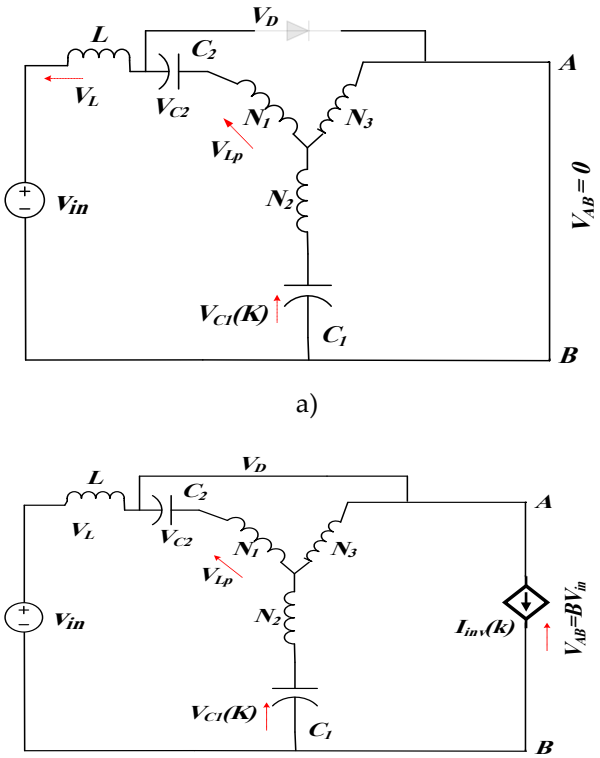

Fig.7: (a) Shoot-through states of qYSI.
(b) Non-Shoot-through states of qYSI.

The capacitor voltage:

$$V_{c1}(K) = V_{dc} + \frac{n1+n3}{n1} * V_{Lp} - \frac{n1+n2}{n1} * V_{Lp} \quad (6)$$

Equation (6) can be rearranged as:

$$V_{c1}(K) = V_{dc} + \left(\frac{n1+n3}{n1} - \frac{n1+n2}{n1}\right) * V_{Lp} \quad (7)$$

$$C_1 \frac{dvc_1(K)}{dt} = V_{dc} - \left(\frac{n3-n2}{n1}\right) * V_{Lp} \quad (8)$$

$$C_1 \frac{v_{c1}(K+1) - v_{c1}(K)}{Ts} = V_{dc} - \left(\frac{n3-n2}{n1}\right) * V_{Lp} \quad (9)$$

3. Model Predictive Control(MPC) for Quazi Y source inverter

The objective of this article is to point out and comment upon MPC of quasi Y-Source Inverter under uncertainty conditions and problems concerning topics coated within changes in the operating conditions and model uncertainties. This issue is referred to as robust stability and has received considerable consideration in scholarly research. A significant purpose for the unguis of model predictive control is the actuality that, In the robust model plan formulation an uncertain added substance time-changing mistake is acquainted with representing model vulnerability coming

about from plant model mismatch caused by unmeasurable disturbances or cycle nonlinearities. In large systems, it is necessary to control the use of feedback to obtain optimal performance and accurate performance when any change occurs in the system inputs, such as the input voltage or the outputs of the system under load. The predictive controller is one of the most important controllers used in electrical systems, which gives optimal stability even in the presence of uncertainty, which complicates the development of a robust model of predictive control. The using of MPC gives a lot of benefits such as: [18]

- In one cost function, the control can guide a lot of variables.
- There is no need for modeling the system as PI and PID controllers.
- It has high reference tracking capability.
- It works with high efficiency even if the parameters are uncertainties
- non-minimum phase effect is reduced or removed at the dynamic change.

The MPC has been used to control several variables, in this paper this control is used to control the inductor current, capacitor voltage, and output currents.

Equations (1)-(3) can be discretized by using Euler discretization as:

$$L\frac{i(K+1)-i(K)}{Ts} = V_{in} + V_{c2} - V_{c1}(K) * \left(1+\frac{n1+n2}{n3-n2}\right) + r_l i_l \quad (10)$$

$$I_L(K+1) = \frac{TS}{L} * (V_{in} + V_{c2} - V_{c1}(K) * \left(1+\frac{n1+n2}{n3-n2}\right) + r_l i_l) \quad (11)$$

$$C_1 \frac{V_{c1}(K+1)-V_{c1}(K)}{Ts} = \left(\frac{n3-n2}{n1}\right) * L_p \frac{di}{dt} \quad (12)$$

$$V_{c1}(K+1) = \left[\frac{L_p}{C_1} * \frac{n3-n2}{n1} * i(K+1) - i(K)\right] + V_{c1}(K) \quad (13)$$

Also equation (4)-(9) Using Euler discretization can be presented as:

$$I_L(K+1) = \frac{TS}{L} * (V_{in} - V_{c1}(K) + (1-\frac{n1+n2}{n1+n3}) * V_{c2} + r_l i_l) \quad (14)$$

$$V_{c1}(K+1) = V_{dc} * \frac{TS}{C_1} - \left[\left(\frac{n3-n2}{n1}\right) * \frac{L_p}{C_1} * i(K+1) - i(K)\right] + Vc1\,(K) - i\_inv\,(K) \quad (15)$$

where, L, and C_l are YZSI network inductance, capacitance, r_l is the internal resistance of the input inductor, V_{in} is a dc voltage source, $i_{inv}(K)$ is the inverter output current. and $i_{inv}(K) = (i_a(K).S_a + i_b(K).S_b + i_c(K).S_c)$, L_p the leakage inductance is seen from the primary , $V_{c1}(K)$ is the capacitor voltage at (K) instant, $i_{a,b,c}(K)$, are the currents of phases a,b,c, and I_L is the input inductor current of L. Also $I_L(K+1)$,$V_{c1}(K+1)$ the Predict input inductor current, and predict capacitor voltage respectively.

The predicted output current can be preset according to Euler discretization

$$i_o(K+1)_{(\alpha,\beta)} = \frac{L_{load}\ i_o(k)_{(\alpha,\beta)} + TS*V_i\ (K+1)}{L_{load} + R_{load}*TS} \quad (16)$$

Minimize errors in the signals to be controlled are collected in one cost function as :

$$g(X) = \left|i_{\alpha_{ref}}(K+1) - i_{\alpha_0}(K+1)\right| + \left|i_{\beta_{ref}}(K+1) - i_{\beta_0}(K+1)\right| + \lambda_{vc}\left|V_{c_{ref}}(K+1) - V_{c1}(K+1)\right| + \lambda_L\left|I_{L_{ref}}(K+1) - I_L(K+1)\right| \quad (17)$$

where λ_{vc} and λ_L the weighting factor for the capacitor voltage and inductor current respectively, $i_{\alpha\_o}(k+1)$, $i_{\beta\_o}(k+1)$ are real/imaginary predicted current vectors and $i_{\alpha\_ref}(k+1)$, $i_{\beta\_ref}(k+1)$ are real/imaginary predicted reference currents; v_{c_ref} and $v_{c1}(k+1)$ are the reference and predicted capacitor voltage. In this paper, the values of weighting factors are chosen by trial and error.

The Relationship Between The Switching States and voltage vectors in each state is presented in Table II

TABLE II THE SWITCHING STATES AND VOLTAGE VECTORS.

Sa	Sb	Sc	Voltage Vector V
1	0	0	$V1 = \frac{2}{3}Vdc$
1	1	0	$V2 = \frac{1}{3}Vdc + j\frac{\sqrt{3}}{3}Vdc$
0	1	0	$V3 = -\frac{1}{3}Vdc + j\frac{\sqrt{3}}{3}Vdc$
0	1	1	$V4 = -\frac{2}{3}Vdc$
0	0	1	$V5 = -\frac{1}{3}Vdc - j\frac{\sqrt{3}}{3}Vdc$
1	0	1	$V6 = \frac{1}{3}Vdc - j\frac{\sqrt{3}}{3}Vdc$
1	1	1	V7= 0
0	0	0	
all shoot-through states			V8= 0

4. Simulation Results

The prototype of Quazi Y-Source is validated via MATLAB/SIMULINK software. the validation will be achieved under dynamic output load based on MPC calculation for qYSI, MATLAB solver is chosen to be the

fixed-advance size with the Ts (10μS). the parameter is listed in Table III. An appropriate value for the weight factor was used, which was deduced by trial and error. Therefore, the value of the weight factor λ_L equal 15.2 value, also λ_{vc}=0.8

TABLE III QYS INVERTER AND LOAD PARAMETERS

Parameter	Value
Rated Power (P_o)	300W
Input DC voltage (V_{in})	50 V
Input inductor (L_{in})	3.5 mH
YZSI network capacitors (C_1, C_2)	490μF, 150μF
leakage Inductance *Lp*	1 μH (see from N1)
Filter resistance (R_f)	10 Ω
Filter inductance (L_f)	5 mH
Switching frequency(f_s)	10 kHz
Sampling time (T_s)	10 μsec
Turns ratio of Coupled inductor (*N1:N2: N3*)	45:30:15= (3:2:1) On C055710A2 MPP core

The performance of the inverter has been validated under steady state as shown in Fig. 5 at 300 W with 0.15 shoot-through duty ratio and $\partial = 5$, as shown in Fig. 8(a) the steady state value of the inductor current is 6.5 A, however, the value of steady state capacitor voltage for Vc1 is 234.2 V capacitor voltage V_{c2} is 185 V as shown in Fig.8(b). In addition, the pulsated DC link voltage reached to 281.85 V (peak) with a boost factor of 5.64 as shown in Fig.9(a). it is worth mentioning that the load is RL load so the output line voltage is not a sinusoidal wave as shown in Fig.9(b).

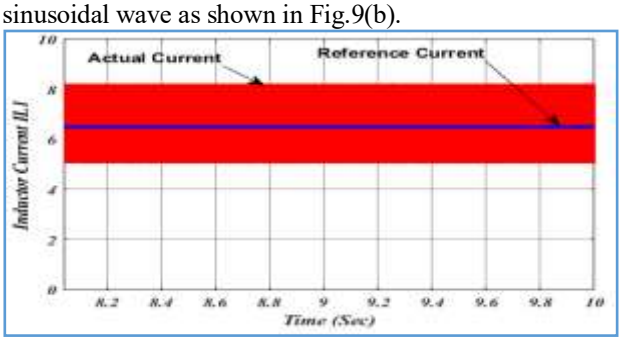

(a)

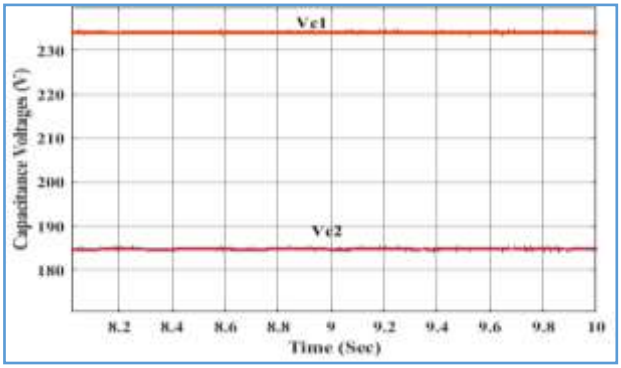

(b)

Fig.8: the signal waveforms for (a) inductor current Input (I_L),(b) voltages for Capacitors V_{C1}, and V_{C2}

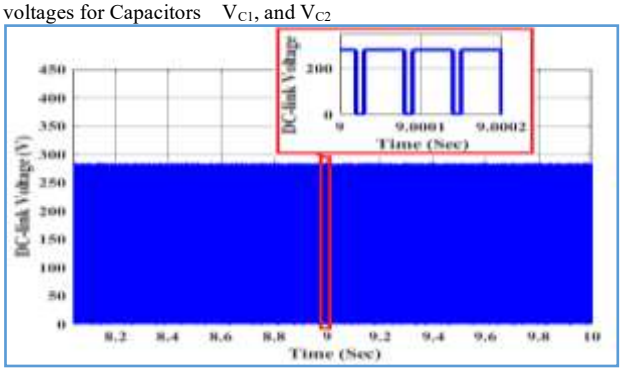

(a)

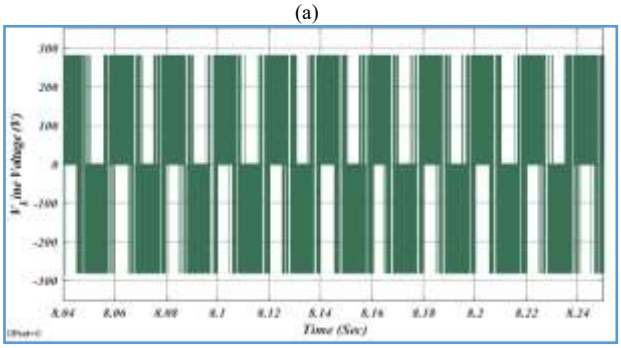

(b)

Fig.9: the signal waveforms for (a) DC-linked voltage (V_{dc}). (b) The line to Line Voltage (V_{L-L})

The second stage is to validate the inverter under dynamic load change which appears in Fig.10. the power is changed from 400W to 300W at t=8s, the inductor current follows the reference value with an average current of 8A before load change to 6.5 A after load change as presented in Fig.10(a). Fig.10 (b) shows the behaviour of output load currents under power change, it is seen that the actual current follows the reference current and changes from 3 A to 2.2 A. On the other hand, the controller succeeded in maintaining the stability of the capacitor voltage V_{C1} at a value of 234.2V, as shown in Fig.10 (c) during the dynamic load, as well as the pulsated voltage Vdc remains constant as the capacitor voltage V_{C1}. remain constant. as shown in Fig. 10(d).

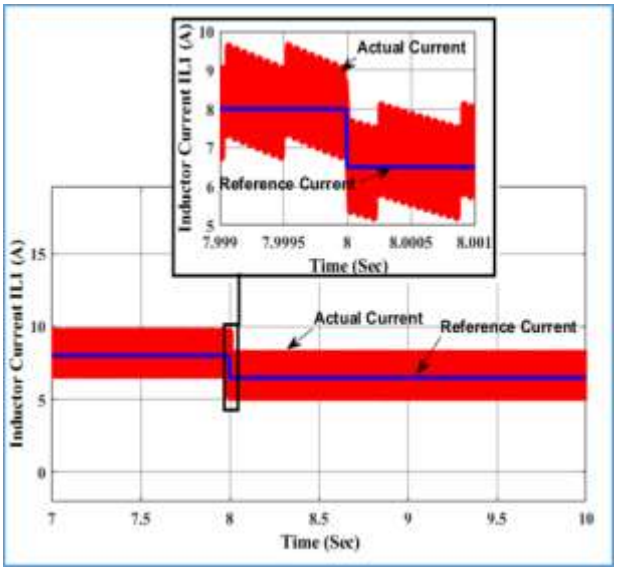

(a)

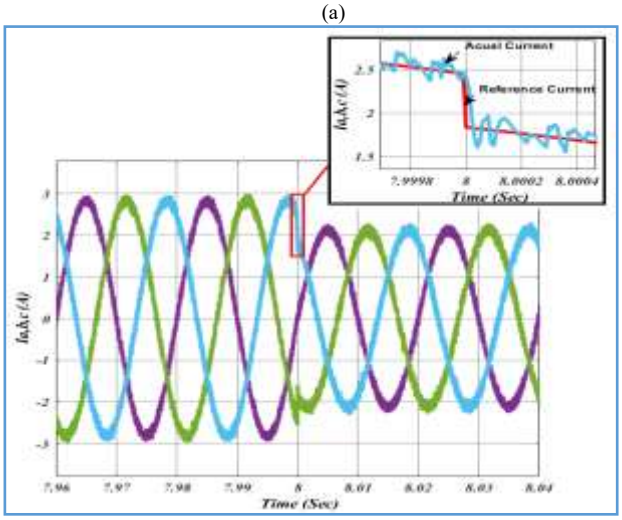

(b)

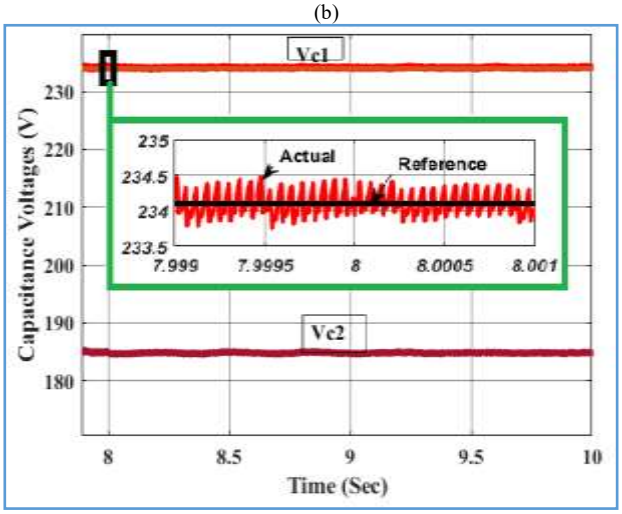

(c)

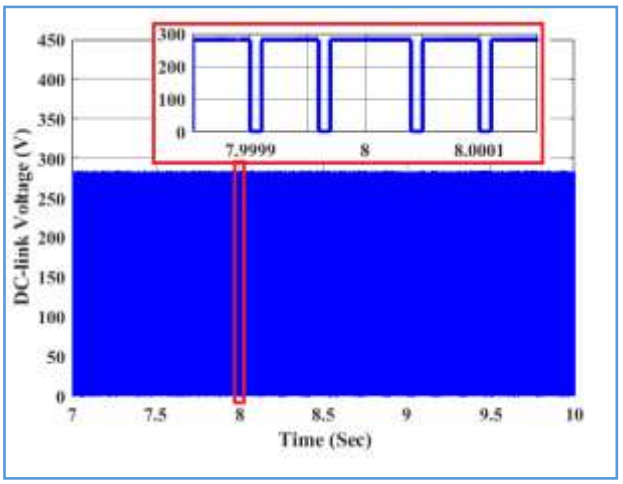

(d)

Fig.10: results under load disturbance (a) Input inductor current (I_L), (b) output current (Io), (c) voltage on Capacitors (V_{C1}, V_{C2}) (d) DC-linked voltage (Vdc).

The third stage of validating the control algorithm is to check the system against the uncertainties the value of the inductor is reduced from 3500µ H to 3350µH. Fig. 11 shows that the system is robust against uncertainties of inductor change.

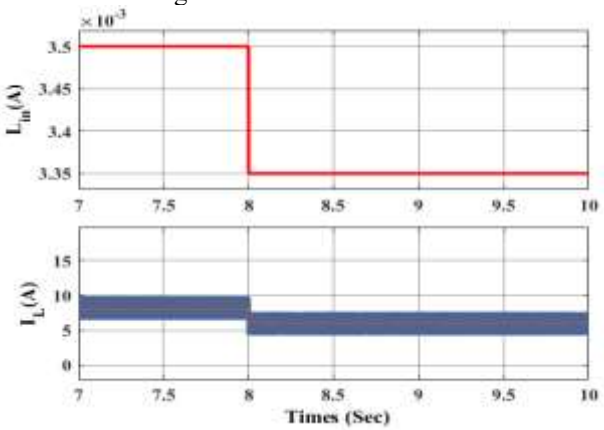

Fig. 11: performance of inductor current under inductance change

Another check has been performed under capacitance change which is shown in Fig. 12. The system has been validated under a change of capacitance from 490µF-470µF

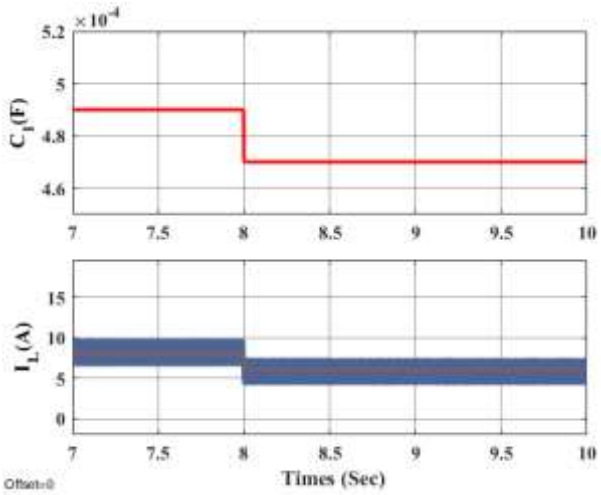

Fig. 12: performance of inductor current under capacitance change

1. Conclusions

A Group of differential Y -Source DC-AC inverters such as Y-source inverters, Extended quasi Y-Source inverters, and quasi Y-Source inverters is presented in this article. Design steps for the control algorithm with the RL Load inverter have been presented comprehensively. A step-up software modulation system has been implemented based on MATLAB Simulink. The theoretical modulation was discussed first and its validation via MATLAB Simulink, The results show that the Model Predictive Controller (MPC) improves performance with high speed when operating conditions change. the inverter. The system is validated under load change the system MPC has been proposed to achieve a good dynamic performance. In addition, the control algorithm has been checked for the system against the uncertainties, where the value of the inductor has been changed and also the value of the capacitor, The results proved the extent of efficiency and the response of the proposed algorithm to control the Y -Source and the absence of any effect on the value of the coil and the capacitor.

References

[1] IRENA, https://www.irena.org/-/media/Files/IRENA/Agency/Publication/2022/Jul/IRENA_Power_Generation_Costs_2021_Summary.pdf "

[2] U.S. Energy Information Administration " https://www.eia.gov/todayinenergy/detail.php?id=46416."

[3] Dogga, R., & Pathak, M. K. (2019). Recent trends in solar PV inverter topologies. Solar Energy, 183, 57-73.

[4] Fang Zheng Peng, "Z-source inverter," in IEEE Transactions on Industry Applications, vol. 39, no. 2, pp. 504-510, March-April 2003, doi: 10.1109/TIA.2003.80892.

[5] de Oliveira-Assis, L., Soares-Ramos, E. P., Sarrias-Mena, R., García-Triviño, P., González-Rivera, E., Sánchez-Sainz, H., ... & Fernández-Ramírez, L. M. (2022). Simplified model of battery energy-stored quasi-Z-source inverter-based photovoltaic power plant with Twofold energy management system. Energy, 244, 122563.

[6] Nguyen, M. K., Lim, Y. C., & Cho, G. B. (2011). Switched-inductor quasi-Z-source inverter. IEEE Transactions on Power Electronics, 26(11), 3183-3191.

[7] Ismeil, M. A., Kouzou, A., Kennel, R., Abu-Rub, H., & Orabi, M. (2012, September). A new switched-inductor quasi-Z-source inverter topology. In 2012 15th International Power Electronics and Motion Control Conference (EPE/PEMC) (pp. DS3d-2). IEEE.

[8] Junjun, L., Daiwei, T., Bowei, X., Chong, L., & Jingyu, Y. (2022). Double-integral sliding mode control of the switched-inductor quasi-Z source boost converter. Measurement and Control, 00202940221110936.

[9] Ismeil, M., Kennel, R., & Abu-Rub, H. (2014). Modeling and experimental study of three-phase improved switched inductor Z-source inverter. EPE journal, 24(4), 14-27.

[10] Laali, S., Babaei, E., & Aalami, M. (2022). Half-bridge Z-source inverter based on T-source configuration with continuous input current and a high boost factor. International Journal of Circuit Theory and Applications.

[11] Y. P. Siwakoti, G. E. Town, P. C. Loh, and F. Blaabjerg, "Y-source inverter," in 2014 IEEE 5th International Symposium on Power Electronics for Distributed Generation Systems (PEDG), Galway, Ireland, Jun. 2014, pp. 1–6, doi: 10.1109/PEDG.2014.6878657.

[12] Y. P. Siwakoti, F. Blaabjerg, and P. C. Loh, "Quasi-Y-source inverter," in 2015 Australasian Universities Power Engineering Conference (AUPEC), Wollongong, Australia, Sep. 2015, pp. 1–5, doi: 10.1109/AUPEC.2015.7324804.

[13] Harinaik, Sugali, and Shelas Sathyan. "Design and Analysis of Quasi-Y Source High Gain DC/DC Resonant Converter for Renewable Energy Applications." Distributed Generation & Alternative Energy Journal (2023): 569-594.

[14] C. Bharatiraja, S. Raghu, A. Raj, and P. Kumar, "Analysis and Simulation of Magnetically Coupled Y Shape Impedance Source Inverter," Indian J. Sci. Technol., vol. 9, no. 44, Nov. 2016, doi: 10.17485/ijst/2016/v9i44/95011.

[15]M. Forouzesh, A. Baghramian, and N. Salavati, "Improved Y-source inverter for distributed power generation," in 2015 23rd Iranian Conference on Electrical Engineering, Tehran, Iran, May 2015, pp. 1677–1681, doi: 10.1109/IranianCEE.2015.7146488.

[16]Y. Ji, L. Hongchen, L. Geng, F. Li, and P. Wheeler, "An Improved Coupled-Inductor Impedance Source Network With More Freedom in Winding Match," IEEE Access, vol. 8, pp. 141472–141480, 2020, doi: 10.1109/ACCESS.2020.3013103.

[17] Liu, H., Li, Y., Liu, K., Loh, P. C., Wang, W., Xu, D., & Blaabjerg, F. (2019). Extended quasi-Y-source inverter with suppressed inrush and leakage effects. IET Power Electronics, 12(4), 719-728.

[18]O. Abdelaal, M. A. Ismeil, and M. Orabi, "Model Predicitve Control Of Quasi Y-Source Inverter," in 2019 21st International Middle East Power Systems Conference (MEPCON), Cairo, Egypt, Dec. 2019, pp. 478–483, doi: 10.1109/MEPCON47431.2019.9007960.